Upgrading of heavy oil by dispersed biogenic magnetite catalysts

DOI:
10.1016/j.fuel.2016.08.015

Document Version
Accepted author manuscript

Upgrading of heavy oil by dispersed biogenic magnetite catalysts

Ashley R. Brown[a1], Abarasi Hart[b], Victoria S. Coker[a], Jonathan R. Lloyd[a*] and Joseph Wood[b*]

[a] Williamson Research Centre for Molecular Environmental Science, School of Earth, Atmospheric and Environmental Sciences, University of Manchester, Manchester, M13 9PL, United Kingdom.

[b] School of Chemical Engineering, University of Birmingham, Edgbaston, Birmingham, B15 2TT, United Kingdom.

[1] Present address: Eawag, Swiss Federal Institute of Aquatic Science and Technology, 8600 Duebendorf, Switzerland. Email: ashley.brown@eawag.ch

* Corresponding authors: ashley.r.brown@manchester.ac.uk; jon.lloyd@manchester.ac.uk; j.wood@bham.ac.uk

Keywords

THAI, CAPRI, magnetite, palladium, catalyst, heavy oil

Abstract

In situ catalytic upgrading of heavy oil offers significant cost savings and overcomes logistical challenges associated with the high viscosity, low API gravity and high molecular weight fractions of unconventional hydrocarbon resources. The THAI-CAPRI process (toe-to-heel air injection – catalytic upgrading process in situ) offers one such route to upgrading through the use of high surface area transition metal cracking catalysts surrounding the production well. Here, we describe the catalytic upgrading of heavy oil in a stirred batch reactor by a

biogenic nanoscale magnetite (BnM; Fe_3O_4). A 97.8% decrease in viscosity relative to the feed oil was achieved and coking was lower compared to thermal cracking alone (6.9 wt% versus 10.2 wt%). The activity of this catalyst was further enhanced by a simple one-step addition of surface associated Pd to achieve loadings of 4.3, 7.1 and 9.5 wt% Pd. This led to significant decreases in viscosity of up to 99.4% for BnM loaded with 9.5 wt% Pd. An increment of 7.8° in API gravity with respect to the feed oil was achieved for 9.5 wt% Pd-BnM, compared with thermal cracking alone (5.3°). Whilst this level of upgrading was comparable to commercially available and previously tested catalysts, significant decreases in the coke content (3 wt% for 9.5 wt% Pd-BnM versus 10 wt% for thermal cracking) and associated increases in liquid content (~90 wt% for 9.5 wt% Pd-BnM versus ~79 wt% for thermal cracking) demonstrate the potential for the use of Pd-augmented biogenic magnetite as a catalyst in the THAI CAPRI process.

1. Introduction

Continuing depletion of global oil reserves has led to unconventional oil resources, such as oil sands, heavy oil and bitumen becomingly increasingly attractive for exploitation. However, heavy oil and bitumen have the disadvantage of high viscosity, low API (American Petroleum Institute) gravity and high molecular weight fractions. This presents a challenge, as the transportation of these materials is both costly and energetically expensive, with heating of the pipeline or solvent addition often required to improve flow rates [1]. Furthermore, conventional oil refineries require heavy oil and bitumen to be first upgraded to a light crude oil before being distilled [2]. Again, this carries associated costs and hence previous exploitation of these resources has been limited.

This demand for enhanced oil recovery (EOR) has led to the development of in situ upgrading technologies [3]. These present the key advantage that upgrading occurs down-hole, thus, enhancing both production and oil quality whilst precluding the need for a secondary surface upgrading facility. In addition, several environmental benefits are offered as unwanted contaminants or by-products are retained in the reservoir, including heavy metals, sulphur and carbon dioxide [4].

The THAI-CAPRI process (toe-to-heel air injection; catalytic upgrading process in situ) is one such technique that combines thermally enhanced oil recovery with in situ catalysis of the heavy oil being mobilised [5–7]. First, in situ combustion is advanced by the continuous injection of air through a vertical well (THAI), which allows the combustion front to be sustained. Second, the CAPRI add-on involves the addition of a catalyst to the horizontal production well, which promotes upgrading of the mobilised oil, e.g. via hydrocracking and hydrodesulfurization. However, challenges arise from the use of fixed bed catalysts due to severe deposition of coke, asphaltenes and metals leading to catalyst deactivation [8,9].

Alternatively, dispersed submicron and nano-particulate catalysts may circumvent this by presenting a larger surface area distributed throughout the site of combustion, and hence, overcoming diffusion limitations and pore plugging associated with fixed bed catalysts, which may obstruct production lines [10–12]. Previous work has shown that dispersed micrometer sized Co-Mo/Al_2O_3 showed superior upgrading compared to its millimetre sized pelleted counterpart [10]. Significant upgrading has also been described for dispersed nanoparticulate hematite and several un-supported transition metal nanoparticles, namely MoS_2, NiO and Fe_2O_3 [11,13]. Although the extent of upgrading was modest compared to thermal cracking, these dispersed materials significantly suppressed coke formation, with

69 the remaining coke having a sponge-type character which may find use as an industrial fuel
70 compared with typical coke materials generated from thermal cracking. These studies
71 highlight the potential for the combination of dispersed nano-sized catalysts with the in situ
72 upgrading offered by the CAPRI process, as an alternative to previously used pelleted
73 hydroprocessing catalysts.

74 Noble metals, such as palladium and platinum also exhibit catalytic upgrading of oil through
75 the promotion of hydrogenation and hydrogenolysis reactions which add hydrogen to the
76 oil molecule (hydrocracking) [14–16]. Supported-Pd catalysts are particularly effective, as
77 the surface area of the palladium is maximised by a nanoparticulate support structure.
78 Typically, this has been done with carbon, silica, alumina and recently bacterial biomass
79 [14,16,17]. Indeed, the use of bacteria in nanocatalyst production represents a more
80 environmentally benign synthesis route.

81 Further work using bacteria has demonstrated the synthesis of magnetic iron oxide
82 nanoparticles using Fe(III)-reducing bacteria such as *Geobacter sulfurreducens* [18,19].
83 Biogenic nanoscale magnetite (bionanomagnetite; BnM) has a large surface area, high
84 chemical reactivity and exhibits effective reduction of a range of organics and metals, being
85 notably more efficient at reducing Cr(VI) than a commercially available synthetic Fe_3O_4
86 [20,21]. Importantly, the particle size of this potential catalyst support can be manipulated
87 during its microbial synthesis, permitting its optimization for novel uses during scalable
88 production [22].

89 Furthermore, biogenic magnetite is very amenable to surface functionalization with other
90 transition metals such as palladium, mediated by reactive surface Fe(II) and an organic layer
91 facilitating reductive precipitation and attachment of Pd(0) [19]. Pd-biomagnetite is highly

reactive toward Cr(VI) and is efficient in hydrogenation of nitroaromatic hydrocarbons and halogenated solvents [21,23,24]. Additionally, when tested in a Heck reaction, coupling iodobenzene to ethyl acrylate or styrene, reaction rates using Pd-biomagnetite were superior or equal to an equimolar amount of commercially available colloidal Pd catalyst [19]. Although Pd is expensive to apply in an oil upgrading process, the cost could potentially be reduced by utilising metal recovered from secondary sources such as electronic waste, scrap catalytic converters or even low grade road dust, which contains traces of platinum group metals exhausted from automotive catalysts [25,26]. In addition, the use of magnetite as a support offers the potential for magnetic recovery and reuse of the catalyst; a major drawback for other precious metal catalyst supports [27].

In light of the previously reported catalytic properties of Pd-bionanomagnetite, and its amenability for optimization for a range of novel uses, this study aimed to assess the catalytic upgrading of oil by biogenic magnetite supported Pd. The upgrading properties of biogenic magnetite alone, as a potential non-functionalised nano-dispersed transition metal catalyst, were also examined. Extents of oil upgrading were assessed in terms of viscosity and API gravity, whilst true boiling point distributions and liquid, gas and coke mass distributions provided important information on oil yields and catalyst efficacy.

1. Material and Methods

2.1. Bionanomagnetite (BnM) catalyst preparations.

Biogenic magnetite was synthesised by the dissimilatory reduction of Fe(III) in a ferrihydrite suspension, by late-log phase cultures of *Geobacter sulfurreducens* as described previously [19,23,24,28,29].

First, ferrihydrite was synthesised by the rapid hydrolysis of a 0.6 M Fe(III) chloride solution via the dropwise addition of 1 M NaOH to pH 7, whilst stirring vigorously [30]. The resultant precipitate was washed six times by centrifugation at 5000*g* for 20 min, followed by removal of the supernatant and resuspension in 18 MΩ de-ionised water.

A culture of *G. sulfurreducens* was grown in a modified freshwater basal medium containing 20 mM acetate and 40 mM fumarate as electron donor and acceptor respectively [31]. Cultures were grown to late log-early stationary phase at 30°C under an 80:20 N_2-CO_2 atmosphere [31]. Cells were then harvested by centrifugation at 5000*g* for 20 min and washed three times in sterile 30 mM $NaHCO_3$ at pH 7.

For magnetite production, 1 L of autoclaved medium was prepared containing 20 mM acetate, 100 mM Fe (as ferrihydrite), 30 mM $NaHCO_3$ and 10 µM anthraquinone-2,6-disulfonate (AQDS) as an electron mediator. As before, the medium was sparged with an 80:20 N_2-CO_2 gas mix and adjusted to pH 7. A suspension of the harvested *G. sulfurreducens* culture was added to a final optical density (at 600 nm) of 0.6. The preparation was then incubated at 30 °C for two days in the dark, during which a black magnetic precipitate was produced. This precipitate was then magnetically separated and washed 3 times in 18 MΩ de-ionised water to remove bacterial cells. The production and purity of the magnetite was confirmed by powder X-ray diffraction (XRD) using a Bruker D8 Advance instrument with Cu $K_{\alpha 1}$ radiation. Transmission electron microscopy (TEM) analysis was performed using a Philips microscope equipped with a 200 keV field emission gun and Gatan imaging filter (GIF200). Samples were prepared by suspending in ethanol prior to drop-casting onto holey carbon support films (Agar Scientific).

2.2. Functionalization of biogenic magnetite with palladium.

The surface of biogenic magnetite crystallites was functionalized with various wt% Pd loadings (% Pd by mass of BnM) according to methods described previously [19,23]. Precipitation of Pd onto magnetite was achieved via surface Fe(II)-mediated reductive precipitation from a N_2 sparged solution of $Na_2Pd(II)Cl_4$. Bottles containing the magnetite suspended in Pd(II)-containing solutions were agitated on rollers for 12 h in the dark. Excess ions were then removed by washing three times in 18 MΩ de-ionised water under an N_2 atmosphere. Suspensions were then re-suspended in acetone so that the suspensions would be miscible with the oil for reactor tests. Prior to testing, 1 mL aliquots were removed, centrifuged at 5000*g* for 5 min and the supernatant aliquots were analysed by ICP-AES to confirm the removal of Pd from solution. The remaining solid material was digested in 3 M HCl and again analysed by ICP-AES to determine the final Fe concentrations and Pd wt% loadings achieved.

2.3. Optimization of Pd loading and reactivity on BnM.

To optimize the wt% Pd loading and reactivity on magnetite surfaces, materials were produced as before but with the inclusion of H_2 sparging steps, followed by the addition of Fe(II) aqueous solutions in order to increase surface-sorbed Fe(II). These two steps aimed to provide excess electron donors for the enhanced reductive precipitation of Pd on to the magnetite surfaces. First, magnetite suspensions were dispersed by sonication in a water bath for 5 min and then sparged with H_2 for 1 min. A 1 mL solution of N_2 sparged 100 mM $Fe(II)SO_4{\cdot}7H_2O$ was then added to the suspensions, followed by sonication for 5 mins and sparging with H_2 for 1 min. An N_2 sparged solution of $Na_2Pd(II)Cl_4$ was added, providing sufficient Pd to achieve a loading of 20 wt% Pd. As before, bottles were agitated on rollers for 12 hours in the dark. Finally, the suspensions were washed three times in 18 MΩ de-

161 ionised water, and three times in acetone to suspend the Pd-BnM in an oil miscible solvent
162 and to remove excess ions. Pd loadings were confirmed as described above.

163 **2.4. Reactor tests.**

164 The heavy oil used in this study was supplied by Petrobank Energy and Resources Ltd (now
165 Touchstone Exploration Inc.), Canada. The initial API gravity and viscosity were 13.9˚ and
166 952 mPa·s. Prior to addition of the Pd-BnM preparations to the batch catalytic reactor, the
167 suspensions were shaken, vortexed for 30 s, sonicated in a water bath for 5 min after which
168 an aliquot was rapidly added to the reactor.

169 **2.5. Reactor conditions.**

170 Upgrading experiments were carried out in a 100 mL capacity stirred batch reactor
171 (Baskerville, United Kingdom) using an experimental procedure described in detail
172 previously [10,32]. The experimental conditions, chosen to match typical *in situ* combustion
173 conditions for the THAI process, were as follows: 425 °C, 20 bar initial pressure (N_2), 500
174 rpm stirring speed, 15 g oil with a 1 mg g^{-1} catalyst-to-oil ratio and a 30 min reaction time.
175 The experiments were also carried out for thermal upgrading alone (without catalyst) and
176 with addition of biomagnetite without palladium as control conditions.

177 **2.6. Analysis of oil.**

178 Before and after upgrading tests, an advanced rheometer AR 1000 (TA Instruments Ltd,
179 United Kingdom) was used to measure oil viscosity, an Anton Paar DMA 35 density meter
180 was used to determine the density and API gravity, and the True Boiling Point (TBP)
181 distribution was obtained using an Agilent 6850N gas chromatograph (GC) in accordance
182 with the ASTM D2887 standard test method. Macromolecules, such as resins and
183 asphaltenes, cannot be accounted for in this method, since the calibration mix contained

only hydrocarbons from C_5 to C_{40}). A detailed description of these instruments and techniques can be found in [9,32,33].

The portion of the carbonaceous deposit after reaction that represented coke was determined using thermogravimetric analysis (TGA). The carbonaceous deposits left in the reactor, which are a composite of coke, residual oil, asphaltenes and catalyst nanoparticles, were collected and burnt off in a Thermogravimetric Analyser (NETZSCH-Geratebau GmbH, TG 209 F1 Iris®). The analysis was performed using a ramp temperature increase from 25 to 900 °C with an air flow rate of 50 mL min^{-1}. The amount of coke in the deposit was determined from the temperature-weight loss curve. Previous analyses under the same experimental conditions have established the temperatures at which residual oil (25 to 410 °C), resins and asphaltenes (410 to 620 °C) and coke (>620 °C) are burnt-off [32–34]. Upon heating, it is possible that the remaining catalyst may undergo modification, e.g. by oxidation of Pd(0) or oxidation of magnetite to hematite [35]. However, the catalyst/oil ratio of 0.001 used here means that any mass differences due to catalyst phase changes would result in only negligible effects on the recorded mass distributions of reaction products.

The non-condensable gas yields after the upgrading reaction was determined by subtracting the mass of the autoclave contents after reaction from the mass of heavy oil prior to reaction.

3. Results and Discussion

3.1. Characterisation of bionanomagnetite.

The microbial production of nano-scale magnetite was achieved via the respiratory reduction of Fe(III), present as a ferrihydrite “gel”, by anoxic washed cell suspensions of the

subsurface Fe(III)-reducing bacterium *G. sulfurreducens*. Complete conversion to magnetite occurred in less than 24 h. The biosynthesis of a pure magnetite product was confirmed by both TEM and powder XRD (Figure 1). TEM further confirmed that the morphology and particle size (15 to 30 nm) was very similar to that reported previously [19,20,23,29]. The surface area of biomagnetite, generated using the same production methods, has been reported previously by our laboratory as 17.1 m^2 g^{-1} [29]. However, this figure should be regarded as an estimate due to particle aggregation that routinely arises during preparation and measurement using the BET N_2 adsorption method.

Previous studies have demonstrated that the surface of biogenic magnetite can be functionalised with Pd(0) via surface Fe(II)-mediated reductive precipitation from a N_2sparged solution of $Na_2Pd(II)Cl_4$ [19,23]. Initially, two loadings of 4.3 and 7.1wt% Pd were achieved by supplying magnetite with Pd(II) concentrations that should have been sufficient for 5 and 20 wt% Pd, respectively, if all the supplied Pd(II) was reduced. This suggests that 7.1 wt% Pd was the maximum Pd loading achievable via this first method. XRD confirmed that solid phase Pd was associated with the magnetite (Figure 2). Using the same synthesis methods as used here, Coker et al. (2010) report that for bionanomagnetite augmented with 5 mol.% Pd, particles of palladium (approx. 5 nm) were precipitated onto the larger magnetite structures (approx. 20 nm), as observed via TEM.

After further optimization, involving H_2 sparging steps followed by addition of aqueous Fe(II) to magnetite suspensions (described in detail above), a Pd loading of 9.5 wt% Pd was achieved. This increased loading is likely a result of the addition of these reductants, with both H_2 and Fe(II) enhancing the reductive precipitation of Pd onto magnetite surfaces.

Despite an excess of Pd(II) supplied, the final loading of 9.5 wt% Pd likely represents the upper limit of Pd-loading achievable using the protocols described here.

3.2. Catalytic upgrading of oil by palladised biogenic magnetite.

The yield balance between liquid (upgraded oil), gas and coke as well as the upgraded oil API gravity and viscosity relative to the feed oil after upgrading experiments are displayed in Table 1. It can be seen that the liquid and coke yields after upgrading are inversely correlated, as an increase in liquid yield correspond to a decrease in coke yield. Whilst thermal cracking produced the lowest yield of upgraded oil (78.8 wt%) and the highest coke yield (10.2 wt%), catalytic upgrading with bionanomagnetite (BnM) yielded 82.3 wt% upgraded oil and 6.9 wt% coke. Increasing the loadings of palladium (Pd) onto the BnM from 4.3 to 9.5 wt%, led to a corresponding increase in the upgraded oil yield from 82.3 to 89.6 wt%, and a decrease in coke from 6.9 to 3.0 wt%. A similar observation has been reported for thermal cracking relative to catalytic upgrading by Hart et al. [9] and Al-Marshed et al. [13]. It has been reported that thermal cracking proceeds by a free radical mechanism that promotes the precipitation of coke precursors, such as resins and asphaltenes. Consequently, polymerisation and condensation occurs, as the abstraction of hydrogen, methyl, ethyl and other material from deposited polyaromatic species to the gas phase occurs, resulting in significant coke formation. However, previous work has demonstrated that catalysts bearing various transition metals display reduced coke yields and corresponding increases in upgraded oil yields. As such, the addition of BnM augmented with Pd may also exhibit the ability to transfer hydrogen, methyl and other material from the gas into the oil phase [13]. This is consistent with the observation that thermal cracking

alone produced more gas (11 wt%) relative to upgrading by BnM (10.8 wt%) and BnM + 9.5 wt% Pd (7.4 wt%).

Table 1. Mass distributions of liquid, gas and coke, and API gravity and viscosity of oil before and after thermal cracking or reaction with BnM, with and without added Pd. Results for $CoMo/Al_2O_3$ [34] and $NiMo/Al_2O_3$ [36], as typical refinery catalysts are shown for comparison.

Sample	Liquid (wt%)	Gas (wt%)	Coke (wt%)	API gravity (°)	Viscosity (mPa·s)
Feed oil				13.2	1031
Thermal cracking	78.8 ± 0.2	11.0 ± 0.3	10.2 ± 0.6	18.5 ± 0.5	28.3 ± 2.1
Co-Mo/Al_2O_3	80.8 ± 0.1	7.1 ± 0.5	12.2 ± 0.1	23.6 ± 0.2	4.4 ± 1.3
Ni-Mo/Al_2O_3	87.3 ± 0.5	7.7 ± 0.7	5.0 ± 0.8	24.9 ± 0.3	3.7 ± 0.6
BnM	82.3 ± 0.3	10.8 ± 0.2	6.9 ± 0.4	18.7 ± 0.3	22.6 ± 1.7
BnM + 4.3 wt% Pd	85.2 ± 0.2	8.9 ± 0.1	5.9 ± 0.3	20.6 ± 0.3	17.8 ± 1.1
BnM + 7.1 wt% Pd	83.7 ± 0.4	10.9 ± 0.6	5.4 ± 0.2	19.9 ± 0.4	15.6 ± 2.3
BnM + 9.5 wt% Pd	89.6 ± 0.7	7.4 ± 0.3	3.0 ± 0.4	21.0 ± 0.2	5.9 ± 0.8

The viscosity and API gravity of crude oil are properties that determine its value, refine-ability and ease of pipeline transportation. The API gravity of the upgraded oil improved from 13.2^o (feedstock) to 18.5^o (thermal cracking), 18.7^o (BnM only) and 21.0^o (BnM + 9.5

wt% Pd), a 159% increase in the case of the latter. Conversely, the viscosity of upgraded oil decreased significantly from 1031 mPa·s (feedstock) to 28.3 mPa·s (thermal cracking), 22.6 mPa·s (BnM only) and 5.9 mPa·s (BnM + 9.5 wt% Pd), a 99.4% decrease. This magnitude of viscosity reduction is capable of improving production and pipeline transportation owing to the level of fluidity experienced at lower viscosity [37]. Similar improvements in catalytically upgraded oil versus thermally cracked heavy oil using conventional, chemically synthesised catalysts has been reported by Hart et al. [9,32,33]. In the absence of a transition metal oxide catalyst, free radicals lead to adduct formation as a result of the addition reaction between two or more active hydrocarbon chains. This, in turn, leads to the formation of larger molecular weight hydrocarbons, which limits any increase in the API gravity or decreases in viscosity of the produced oil [37,38]. However, the presence of a transition metal oxide catalyst, such as BnM, likely promotes hydrogen-transfer reactions between hydrocarbons in the gas and liquid phases, which helps to cap free radicals once they are formed, thus moderating the adduct formation. The augmentation of BnM with surface associated Pd likely promotes further hydrogenation reactions, which produces significant improvements in API gravity and viscosity of the upgraded oil as the percentage loading of Pd on BnM increases from 4.3 to 9.5 wt%.

The extent of the improvement in API gravity and viscosity with increasing Pd loading may be limited due to the sulfur content of the heavy oil (3.52 wt%). It has been reported that sulfur and sulfur-containing species (e.g. H_2S, RSH, RSSR) may lead to poisoning of Pd-surfaces [39], which may have impeded the activity and performance of the particles. Indeed a similar effect was observed in the testing of palladized iron for the dechlorination of groundwater [40]. The experiments demonstrated that the dechlorination reaction occurred efficiently until the surface of the Pd/Fe became fouled. It was found that reduced

sulfur species could eventually lead to permanent poisoning of the palladium. Contrary to this, other studies have shown that sulfur may prolong the life of platinum group metal catalysts and even promote activity and enhance selectivity [39,41,42]. However this phenomenon is typically noted for sulfur concentrations on catalyst surfaces that are significantly lower than that reported for the bulk sulfur content of the heavy oil used in this study (e.g. <0.5 wt.%). Despite this, the authors of a previous study utilising the same native oil and reactor conditions as used here, assumed that although sulfur is present in potentially inhibitory concentrations, it may be present in non-available forms due to its association with other metals present in the native feed oil [34]. Although the extent of sulphur deactivation was not evaluated in this study, the data suggest that the Pd-BnM catalyst performed comparably with typically refinery catalysts (table 1).

The true boiling point (TBP) distribution curves obtained from simulated distillation (SIMDIS) of the feed oil and oils upgraded by thermal cracking and BnM are presented in Figure 3. The TBP curves show the cumulative volume distilled as a function of temperature. The shift of the TBP curves from reactor tests containing added catalyst to the left of the TBP curve of the feed oil indicate that the upgraded oil contains lighter hydrocarbon components compared to the feed oil.

A noticeable improvement in the amount of distillate obtainable can be observed between the temperature ranges of 230 to 430 ^{o}C, for all reactor tests relative to the feed oil. The TBP curves of the upgraded oils by thermal cracking and BnM only are approximately identical, which is in line with their similar API gravities and viscosities reported in Table 1. However, the addition of Pd to BnM produced a further increase in the amount of distillate fractions distilled between the boiling temperature range of 200 to 450 ^{o}C, with significant

309 increases recorded when the Pd loading of the BnM was increased to 9.5 wt% Pd. This
310 observed increase in naphtha and middle distillate fractions upon the increasing addition of
311 Pd to BnM can be attributed to the enhanced ability of Pd to facilitate hydrogenation
312 reactions, compared with Fe. Hence, the synergistic effect of Fe plus Pd enhanced the
313 conversion of high boiling hydrocarbon components into lighter hydrocarbon fractions,
314 relative to that observed for BnM alone. These trends in TBP curves are in line with the API
315 gravities and viscosities of the upgraded oils, relative to the feed oil, shown in Table 1.

316 **3.3. Outlook and comparison with commercially available catalysts.**

317 In summary, the experiments reported here have demonstrated that both biogenic
318 magnetite augmented with Pd and biogenic magnetite alone are capable of significant
319 catalytic upgrading of oil, as measured by increases in liquid yield, API gravity and
320 corresponding decreases in viscosity. A reduction in coke content and an increase in lighter
321 hydrocarbon fractions further demonstrate the potential for its use as a catalyst in the THAI
322 CAPRI process.

323 Dispersed nanoparticulate magnetite offers increased oil contact through a large surface-
324 area-to-volume ratio and decreased diffusion path lengths compared with using fixed-bed
325 reactors [10,43]. Indeed, the use of biomagnetite as the catalyst support not only offers
326 catalytic properties itself but also provides a large surface area over which the Pd is
327 precipitated, facilitated by the large pool of surface associated Fe(II) that serves as the
328 reductant. As Pd also promotes hydrogenation and hydrogenolysis reactions [14–16], Pd-
329 augmented bionanomagnetite represents a bi-functional catalyst with increased activity and
330 performance.

Indeed, previous studies have shown that commercially available Ni-Mo/Al_2O_3 and dispersed ultrafine Co-Mo/Al_2O_3 achieved a higher API gravity increase than the tested catalysts in this study under the same conditions as used here (23.6 and 22.5° respectively) [34,36]. However, lower coke contents and a higher liquid yield of 89.6 wt% using 9.5 wt% Pd-BnM were achieved in this study, compared with 87.3 and 80.8 wt% for Ni-Mo/Al_2O_3 and dispersed ultrafine Co-Mo/Al_2O_3, respectively. The coke content of 12.15 wt% for Co-Mo/Al_2O_3 was higher than achieved for all the tested materials reported here, and lower coking was achieved using 9.5 wt% Pd-BnM (3.0 wt%) than was reported for Ni-Mo/Al_2O_3 (5.0 wt %). As coke production reduces both the liquid yield and the lifetime of the catalyst [44], decreases in the coke levels achieved by Pd-BnM are a favourable result. However, it is not clear whether such gains in coke reduction are able to off-set the lower levels of API gravity and viscosity achieved.

Similar comparisons can be made with dispersed transition metal catalysts. Fe_2O_3, MoS_2, MoO_3, FeS and NiO have all shown slightly higher levels of upgrading in terms of API gravity (typically ~21°) [11,13]. However, viscosities were all significantly higher for these materials (typically 70 to 140 mPa·s; though this may be due to the slightly different reactor conditions used) and coke levels (>4.3wt% coke) were again, not as low as for 9.5 wt% Pd-BnM (3.0wt% coke).

Recent work has investigated upgrading using nanoparticulate Pd and Pt supported on bacterial cell scaffolds, under the same reactor conditions used here [34,36]. Using similar Pd loadings, the authors achieved very similar improvements in yields, coking and viscosity, supporting our finding that biotechnological approaches to catalyst synthesis can generate commercially competitive catalysts using “green” biosynthesis routes.

Whilst such improvements in oil upgrading by Pd-BnM, compared to those of commercial and other tested materials, may appear modest at the laboratory scale tested here, such incremental changes may lead to significant benefits in process economics at full scale. Recent work has demonstrated that biogenic magnetite production can be successfully scaled up from laboratory to pilot plant-scale whilst controlling its reactivity, magnetic properties and particle size, suggesting that its exploitation in commercial settings are achievable [45]. In addition, the production process may offer a more environmentally benign route to catalyst production than established chemical methods and thus, such environmental benefits may offset the cost of using expensive precious metals, such as palladium [27]. Indeed, recent work suggests that this cost may be further reduced by sourcing metals from electronic waste, scrap catalytic converters or road dust, which contains platinum group metals exhausted from automotive catalysts [25,26]. In this context, the competitive results reported here suggest that an economic cost analysis may be warranted.

Finally, our experiments have relied on the laboratory production of magnetite using a pure culture of a model Fe(III)-reducing bacterium. However, the natural occurrence of such species in sub-surface sediments, alongside native Fe(III)-bearing oxides, may represent the potential for the *in situ* generation of a catalyst. Future experiments will, therefore, focus on achieving the stimulation of such organisms in relevant geological formations and, thus, eliminating the need for delivery of a catalyst to the reaction front of the THAI process. Enhanced oil recovery by such means may further reduce financial overheads associated with the THAI-CAPRI process.

4. Acknowledgements.

Funding: This work was supported by the UK Engineering and Physical Sciences Research Council (EPSRC; grant number EP/J008303/1). The data from this study are available online via epapers.bham.ac.uk. The authors would like to thank Petrobank Energy and Resources Ltd. and Touchstone Exploration Inc., Canada for supplying the heavy oil used in these experiments. We also thank Prof. Lynne Macaskie, University of Birmingham, for advice and helpful discussions; Paul Lythgoe, Manchester Analytical Geochemistry Unit, for ICP-AES analyses; Dr. John Waters for XRD and Dr. Mike Ward, University of Leeds EPSRC Nanoscience and Nanotechnology Facility, for TEM.

5. References

[1] Martinez-Palou R, Mosqueira M de L, Zapata-Rendon B, Mar-Juarez E, Bernal-Huicochea C, de la Cruz Clavel-Lopez J, et al. Transportation of heavy and extra-heavy crude oil by pipeline: A review. J Pet Sci Eng 2011;75:274–82. doi:10.1016/j.petrol.2010.11.020.

[2] Carrillo JA, Corredor LM. Upgrading of heavy crude oils: Castilla. Fuel Process Technol 2013;109:156–62. doi:10.1016/j.fuproc.2012.09.059.

[3] Weissman JG, Kessler R V, Sawicki RA, Belgrave JDM, Laureshen CJ, Mehta SA, et al. Down-Hole Catalytic Upgrading of Heavy Crude Oil. Energy & Fuels 1996;10:883–9. doi:10.1021/ef9501814.

[4] Shah A, Fishwick R, Wood J, Leeke G, Rigby S, Greaves M. A review of novel techniques for heavy oil and bitumen extraction and upgrading. Energy Environ Sci

2010;3:700–14. doi:10.1039/b918960b.

[5] Xia TX, Greaves M. Upgrading Athabasca tar sand using toe-to-heel air injection. J Can Pet Technol 2002;41.

[6] Xia TX, Greaves M, Turta AT, Ayasse C. THAI - A “short-distance Displacement” in situ combustion process for the recovery and upgrading of heavy oil. Chem Eng Res Des 2003;81:295–304. doi:10.1205/02638760360596847.

[7] Greaves M, El-Saghr A, Xia TX. CAPRI horizontal well reactor for catalytic upgrading of heavy oil: Advances in oil field chemistry: Downhole upgrading. Prepr Chem Soc Div Pet Chem 2000;45:595–8.

[8] Shah A, Fishwick RP, Leeke GA, Wood J, Rigby SP, Greaves M. Experimental optimization of catalytic process in situ for heavy-oil and bitumen upgrading. J Can Pet Technol 2011;50:33–47. doi:10.2118/136870-PA.

[9] Hart A, Shah A, Leeke G, Greaves M, Wood J. Optimization of the CAPRI process for heavy oil upgrading: Effect of hydrogen and guard bed. Ind Eng Chem Res 2013;52:15394–406. doi:10.1021/ie400661x.

[10] Hart A, Greaves M, Wood J. A comparative study of fixed-bed and dispersed catalytic upgrading of heavy crude oil using-CAPRI. Chem Eng J 2015;44:1–11. doi:10.1016/j.cej.2015.01.101.

[11] Al-Marshed A, Hart A, Leeke G, Greaves M, Wood J. Optimization of heavy oil upgrading using dispersed nanoparticulate iron oxide as a catalyst. Energy & Fuels 2015;29:6306–16.

[12] Hashemi R, Nassar NN, Pereira Almao P. Nanoparticle technology for heavy oil in-situ

upgrading and recovery enhancement: Opportunities and challenges. Appl Energy 2014;133:374–87. doi:10.1016/j.apenergy.2014.07.069.

[13] Al-Marshed A, Hart A, Leeke G, Greaves M, Wood J. Effectiveness of different transition metal dispersed catalysts for in situ heavy oil upgrading. Ind Eng Chem Res 2015;54:10645–55.

[14] Wood J, Bodenes L, Bennett J a, Deplanche K, Macaskie LE. Hydrogenation of 2-Butyne-1,4-diol Using Novel Bio-Palladium Catalysts. Ind Eng Chem Res 2010;49:980–8. doi:10.1021/ie900663k.

[15] Del Bianco A, Panariti N, Di Carlo S, Elmouchnino J, Fixari B, Le Perchec P. Thermocatalytic hydroconversion of heavy petroleum cuts with dispersed catalyst. Appl Catal A Gen 1993;94:1–16. doi:http://dx.doi.org/10.1016/0926-860X(93)80041-N.

[16] Schüth C, Reinhard M. Hydrodechlorination and hydrogenation of aromatic compounds over palladium on alumina in hydrogen-saturated water. Appl Catal B Environ 1998;18:215–21. doi:10.1016/S0926-3373(98)00037-X.

[17] Chaplin BP, Reinhard M, Schneider WF, Schüth C, Shapley JR, Strathmann TJ, et al. Critical Review of Pd-Based Catalytic Treatment of Priority Contaminants in Water. Environ Sci Technol 2012;46:3655–70. doi:10.1021/es204087q.

[18] Coker VS, Telling ND, van der Laan G, Pattrick RAD, Pearce CI, Arenholz E, et al. Harnessing the Extracellular Bacterial Production of Nanoscale Cobalt Ferrite with Exploitable Magnetic Properties. ACS Nano 2009;3:1922–8. doi:10.1021/nn900293d.

[19] Coker VS, Bennett JA, Telling ND, Henkel T, Charnock JM, van der Laan G, et al. Microbial engineering of nanoheterostructures: biological synthesis of a magnetically

recoverable palladium nanocatalyst. ACS Nano 2010;4:2577–84. doi:10.1021/nn9017944.

[20] Cutting RS, Coker VS, Telling ND, Kimber RL, Pearce CI, Ellis BL, et al. Optimizing Cr(VI) and Tc (VII) remediation through nanoscale biomineral engineering. Environ Sci Technol 2010;44:2577–84.

[21] Watts MP. Novel bionanotechnological approaches for the remediation of contaminated land. University of Manchester, 2014.

[22] Byrne JM, Telling ND, Coker VS, Pattrick RAD, Van Der Laan G, Arenholz E, et al. Control of nanoparticle size, reactivity and magnetic properties during the bioproduction of magnetite by Geobacter sulfurreducens. Nanotechnology 2011;22:455709.

[23] Watts MP, Coker VS, Parry SA, Thomas RAP, Kalin R, Lloyd JR. Effective treatment of alkaline Cr(VI) contaminated leachate using a novel Pd-bionanocatalyst: Impact of electron donor and aqueous geochemistry. Appl Catal B Environ 2015;170-171:162–72. doi:10.1016/j.apcatb.2015.01.017.

[24] Crean DE, Coker VS, van der Laan G, Lloyd JR. Engineering biogenic magnetite for sustained Cr(VI) remediation in flow-through systems. Environ Sci Technol 2012;46:3352–9. doi:10.1021/es2037146.

[25] Murray AJ. Recovery of Platinum Group Metals from Spent Furnace Linings and Used Automotive Catalysts. University of Birmingham, 2012.

[26] Macaskie LE, Mikheenko IP, Yong P, Deplanche K, Murray AJ, Paterson-Beedle M, et al. Today’s wastes, tomorrow's materials for environmental protection. Hydrometallurgy 2010;104:483–7. doi:10.1016/j.hydromet.2010.01.018.

[27] Lloyd JR, Byrne JM, Coker VS. Biotechnological synthesis of functional nanomaterials. Curr Opin Biotechnol 2011;22:509–15. doi:10.1016/j.copbio.2011.06.008.

[28] Cutting RS, Coker VS, Fellowes JW, Lloyd JR, Vaughan DJ. Mineralogical and morphological constraints on the reduction of Fe(III) minerals by Geobacter sulfurreducens. Geochim Cosmochim Acta 2009;73:4004–22. doi:DOI 10.1016/j.gca.2009.04.009.

[29] Watts MP, Coker VS, Parry SA, Pattrick RAD, Thomas RAP, Kalin R, et al. Biogenic nano-magnetite and nano-zero valent iron treatment of alkaline Cr(VI) leachate and chromite ore processing residue. Appl Geochemistry 2015;54:27–42. doi:10.1016/j.apgeochem.2014.12.001.

[30] Lovley DR, Phillips EJP. Organic matter mineralization with reduction of ferric iron in anaerobic sediments. Appl Environ Microbiol 1986;51:683–9.

[31] Lloyd JR, Leang C, Hodges Myerson AL, Coppi M V, Cuifo S, Methe B, et al. Biochemical and genetic characterization of PpcA, a periplasmic c-type cytochrome in *Geobacter sulfurreducens*. Biochem J 2003;369:153–61. doi:10.1042/BJ20020597 BJ20020597 [pii].

[32] Hart A, Leeke G, Greaves M, Wood J. Down-hole heavy crude oil upgrading by CAPRI: Effect of hydrogen and methane gases upon upgrading and coke formation. Fuel 2014;119:226–35. doi:10.1016/j.fuel.2013.11.048.

[33] Hart A, Lewis C, White T, Greaves M, Wood J. Effect of cyclohexane as hydrogen-donor in ultradispersed catalytic upgrading of heavy oil. Fuel Process Technol 2015;138:724–33.

[34] Hart A, Omajali JB, Murray AJ, Macaskie LE, Greaves M, Wood J. Comparison of the

effects of dispersed noble metal (Pd) biomass supported catalysts with typical hydrogenation (Pd/C, Pd/Al2O3) and hydrotreatment catalysts (CoMo/Al2O3) for in-situ heavy oil upgrading with Toe-to-Heel Air Injection (THAI). Fuel 2016;180:367–76.

[35] Cornell RM, Schwertmann U. The iron oxides. Second. Weinheim: WILEY-VCH Verlag; 2003.

[36] Omajali J. Novel bionanocatalysts for green chemistry applications. University of Birmingham, 2015.

[37] Hart A. Advanced studies of catalytic upgrading of heavy oils. University of Birmingham, UK, 2014.

[38] Habib FK, Diner C, Stryker JM, Semagina N, Gray MR. Suppression of addition reactions during thermal cracking using hydrogen and sulfided iron catalyst. Energy & Fuels 2013;27:6637–45.

[39] Dunleavy JK. Sulfur as a catalyst poison. Platin Met Rev 2006;50:110.

[40] Korte NE, Zutman JL, Schlosser RM, Liang L, Gu B, Fernando Q. Field application of palladized iron for the dechlorination of trichloroethene. Waste Manag 2000;20:687–94.

[41] Tong YJ. Unconventional promoters of catalytic activity in electrocatalysis. Chem Soc Rev 2012;41:8195–209. doi:10.1039/C2CS35381D.

[42] McCue AJ, Anderson JA. Sulfur as a catalyst promoter or selectivity modifier in heterogeneous catalysis. Catal Sci Technol 2014;4:272–94. doi:10.1039/C3CY00754E.

[43] Angeles MJ, Leyva C, Ancheyta J, Ramírez S. A review of experimental procedures for heavy oil hydrocracking with dispersed catalyst. Catal Today 2014;220:274–94.

doi:10.1016/j.cattod.2013.08.016.

[44] Forzatti P, Lietti L. Catalyst deactivation. Catal Today 1999;52:165–81. doi:http://dx.doi.org/10.1016/S0920-5861(99)00074-7.

[45] Byrne JM, Muhamadali H, Coker VS, Cooper J, Lloyd JR. Scale-up of the production of highly reactive biogenic magnetite nanoparticles using Geobacter sulfurreducens. J R Soc Interface 2015;12.

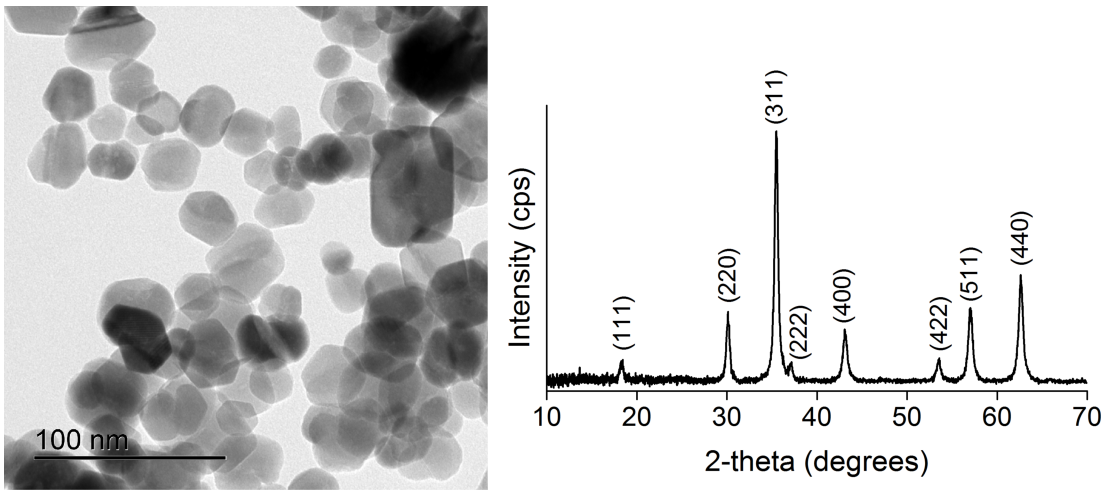

Fig. 1. Bright field TEM and powder XRD diffractogram of biogenic magnetite.

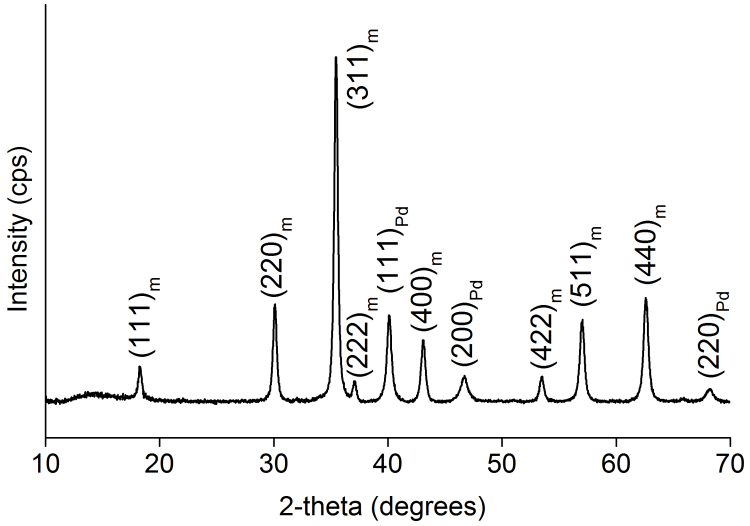

Fig. 2. XRD diffractogram of 9.5 wt. % Pd-coated biogenic magnetite.

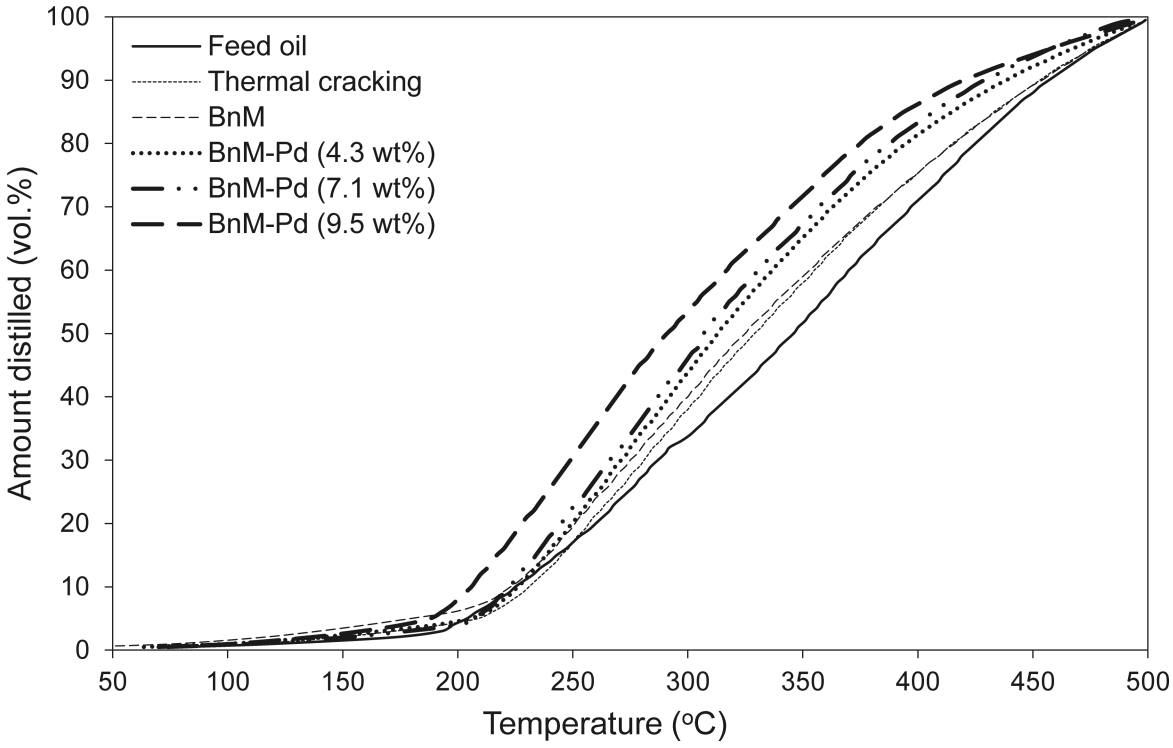

527

528 **Fig. 3.** True boiling point distribution curves of feed and upgraded oils after thermal cracking

529 and after reaction with Pd-coated biomagnetite (BnM).

530